

# The Origin of the Boson Peak and Thermal Conductivity Plateau in Low Temperature Glasses.

Vassiliy Lubchenko and Peter G. Wolynes

*Department of Chemistry and Biochemistry, University of California at San Diego, La Jolla, CA 92093-0371*

(November 13, 2018)

We argue that the intrinsic glassy degrees of freedom in amorphous solids giving rise to the thermal conductivity plateau and the “boson peak” in the heat capacity at moderately low temperatures are directly connected to those motions giving rise to the two-level like excitations seen at still lower temperatures. These degrees of freedom can be thought of as strongly anharmonic transitions between the local minima of the glassy energy landscape that are accompanied by ripplon-like domain wall motions of the glassy mosaic structure predicted to occur at  $T_g$  by the random first order transition theory. The energy spectrum of the vibrations of the mosaic depends on the glass transition temperature, the Debye frequency and the molecular length scale. The resulting spectrum reproduces the experimental low temperature Boson peak. The “non-universality” of the thermal conductivity plateau depends on  $k_B T_g / \hbar \omega_D$  and arises from calculable interactions with the phonons.

PACS Numbers: 65.60.+a, 66.70.+f, 63.20.Ry, 66.35.+a

A multitude of phenomena are observed in all low temperature glasses that can only be explained by the existence of excitations not present in crystals. At very low temperatures, the universal scalings of heat capacity and thermal conductivity suggest these excitations cannot be simply ascribed to the local molecular motions specific to each substance [1,2]. Yet quantitative analysis of the experiments has generally relied on purely phenomenological models that invoke unrelated types of excitations in different temperature regimes. At liquid helium temperatures the excitations of glasses are well described as two-level systems [3–5], but at somewhat higher temperatures the more mysterious “boson peak” appears in the heat capacity and the phonon mean free path falls precipitously, as if new scatterers became active, leading to a plateau in the thermal conductivity. Several different ideas about these additional excitations have been explored, ranging from harmonic excitations of a disordered lattice [6] to anharmonic local modes of a “soft potential” with distributed parameters [7].

In contrast, here we suggest that like the two level systems [8] these quantum excitations in glasses are intrinsic and essential relics of the non-equilibrium character of the glass after it is prepared. We show that quantized “domain wall motions” connected with the mosaic structure of glasses predicted by the random first order transition theory of glasses [9], explain quantitatively the boson peak and conductivity plateau.

The random first order transition theory of the glass transition suggests there is a dynamical mosaic structure in classical supercooled liquids [10]. This mosaic structure is directly manifested in the dynamical heterogeneity observed in supercooled liquids using single molecule experiments [11] and nonlinear relaxation experiments [12]. Below  $T_g$ , the mosaic is spatially defined by the

molecular motions that were not arrested at  $T_g$ , and is thus only dynamically detectable. We have shown these same motions at liquid helium temperatures would be quantized and can be described by the two state system phenomenology. This identification predicts the density of states arising from these motions and accounts for the previously unexplained universality of thermal conductivity in the liquid helium temperature regime. As the temperature is raised, however, the theory indicates these excitations should lose their strict two level character. The predicted temperature of the crossover to multilevel behavior coincides with the temperature regime where further excitable modes have been needed to explain experiments. In this paper, we show explicitly how the number of extra excitable modes of the mosaic accounts quantitatively for the data, thus removing the need to invoke additional mechanisms, although other contributions may well be present to some extent. The excitations in the boson peak, like the two-level systems, active at lower temperatures, turn out to be collective motions of many particles ( $\sim 200$ ) encompassing rearrangements of a typical domain frozen-in at the glass transition. The multilevel behavior of these domains can be pictured as involving the concomitant excitation of the “ripplon” modes of the glassy mosaic along with the transition between local minimum energy configurations of a mosaic cell.

According to the random first order transition theory of supercooled liquids [9], metastable configurations begin to last locally longer than a few vibrations just below a dynamical transition temperature  $T_A$ . Below this transition a glass forming liquid samples exponentially many metastable configurations much higher in energy than those of the corresponding crystal, but which are long lived. Glassy dynamics is described by the activated mo-

tions between minima. The liquid can be visualized as a mosaic of domains which locally resemble low free energy configurations that are separated from each other by frustrated higher energy interfaces, or *domain walls*. The length scale of the mosaic and number density of these walls is determined by the competition between the energy cost of a wall and the entropic advantage of using the large number of configurations. As temperature is lowered the configurational entropy per particle,  $s_c$ , decreases so that the cooperative length grows. This leads to a larger activation barrier that eventually gives relaxation times exceeding the laboratory time scale. The size and rate of motion of these mosaic domains can be calculated without adjustable parameters once the liquid's heat capacity jump at the glass transition is known [10]. In the classical regime this theory leads to predictions of the average barrier and distributions of barriers in quantitative agreement with experiment [13]. According to this microscopic calculation, at the  $T_g$  that corresponds with one hour relaxation time, the size of the cooperative region  $\xi$  is expected to vary only a little from substance to substance. A mosaic cell allows for at least one alternative kinetically accessible configuration at  $T_g$ . These alternate states therefore have spectral density  $\sim 1/T_g$  per domain of size  $\xi^3$  [8]. This agrees with the measured density of two-level systems [5]. While activated at  $T_g$ , below  $T_g$ , motion between these alternative states remains possible, switching to coherent resonant tunneling at a temperature proportional but smaller than the Debye temperature:  $\sim (a/\xi)T_D/2\pi$  [8].

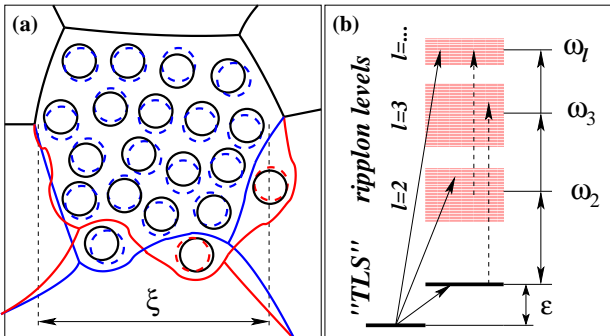


FIG. 1. (a) Schematic of a tunneling mosaic cell is given, with doubled circles denoting atomic tunneling displacements. The boundary's location is variable, as illustrated (in an exaggerated manner) by the blue and red lines. The domain wall distortion amounts to populating ripplon states on top of the structural transition energy  $\epsilon$ , as shown in (b). All transitions exemplified by solid lines involve tunneling between the intrinsic states and are coupled linearly to the lattice distortion and contribute the strongest to the phonon scattering. The "vertical" transitions, denoted by the dashed line, are coupled to the higher order strain; they contribute only to the Rayleigh scattering (which is too weak to account for the plateau [14]).

At low temperatures the two-level system excitations

involve tunneling of the mosaic cells typically containing  $N^* \simeq 200$  atoms. The tunneling path involves stagewise motion of the wall separating the distinct alternative configurations through the cell until a near resonant state is found. At higher temperatures, other final states are possible since the exact number and identity of the atoms that tunnel can vary (see Fig.1a). These new configurations typically will be like the near resonant level but will also move a few atoms at the boundary, i.e. at the interface to another domain. These fluctuations of the domain boundary shape can be visualized as domain wall surface modes ("ripplons"). They cost a surface energy that varies with the size of the domain and have kinetic energy consistent with the mass of the moving domain wall. It is not surprising that the ripplon's frequencies turn out to be proportional to  $\omega_D$ , the basic quantum energy scale in the system just as does the crossover temperature. A detailed calculation of the ripplon spectrum would require a considerable knowledge of the topology and statistics of the mosaic. At each temperature below  $T_A$  the domain wall foam is an equilibrium structure made up of nearly flat patches. According to the random first order transition theory, the effective surface tension depends on the curvature and vanishes at large radius of curvature as  $\sigma(r) \propto r^{-1/2}$ . To approximate the spectrum we notice that the ripples of wavelength larger than the size of a patch will typically sense a roughly spherical surface of radius  $R = \xi(3/4\pi)^{1/3}$ . The surface tension of the mosaic has been calculated from the classical microscopic theory and is given by  $\sigma(R) = \frac{3}{4}(k_B T_g/a^2) \log((a/d_L)^2/\pi e)(a/R)^{1/2}$  [10], where  $d_L/a$  is the universal Lindemann ratio. By itself such a tension would collapse the mosaic but this tension should be compensated by stretching the frozen-in outside walls of neighboring mosaic cells. This compensating effect can be approximated by an isotropic positive pressure of a ghost (i.e. vanishing density) gas on the inside. Calculating the frequencies of the surface eigen-modes of a hollow sphere, subject only to surface tension, is a classic problem of mathematical physics [15]. Accounting for the unusual  $r$  dependence of the surface tension  $\sigma(r) \propto r^{-1/2}$  modifies the standard result for the frequencies by a factor of 9/8. The eigenmodes have frequencies  $\omega_l^2 = \frac{9}{8}(\sigma/\tilde{m}_W R^2)(l-1)(l+2)$ , where  $\tilde{m}_W = (d_L/a)^2 \rho a$  is the domain wall mass per unit area [8] and  $\rho$  is the mass density of the glass. The  $l$ -th mode of a sphere is  $(2l+1)$ -fold degenerate. Using  $k_B T_g \simeq \rho c_s^2 a^3 (d_L/a)^2$  [8], one finds then  $\omega_l \simeq 1.34 \omega_D (a/\xi)^{5/4} \sqrt{(l-1)(l+2)/4} \simeq 0.15 \omega_D \sqrt{(l-1)(l+2)/4}$ . Because of the universality of the  $(a/\xi)$  ratio [10],  $\omega_l$  is a multiple of the Debye frequency. Due to the material's discreteness, there are no harmonics of higher than  $(\frac{3}{4\pi} N^*)^{1/3}$   $[(R - a/2)/R] \simeq 9..10$ th order, a relatively large number, which makes the continuum approximation plausible. The lowest allowed ripplon mode is  $l = 2$ , and has a frequency of  $\sim 1$ THz for

silica. This is in agreement with the Boson peak in the inelastic neutron scattering data [16]).  $l = 1$  corresponds to a domain translation and is accounted for by the underlying phonon momentum non-conserving tunneling transition itself. The  $l = 0$  is a uniform domain dilation relevant to aging below  $T_g$ . The existence of the domain wall vibrations lets us visualize the multilevel character of the tunneling centers as exhibited at temperatures above the TLS regime. A schematic of the resultant droplet quantized energy levels is shown in Fig.1b.

The (classical) density of energy minima of a domain is  $n(\epsilon) = \frac{1}{k_B T_g} e^{\epsilon/k_B T_g}$  [8], where the energy zero corresponds to the (high-energy) configuration frozen-in at  $T_g$ . The negative  $\epsilon$ 's correspond to some of the very numerous but mostly unavailable lower lying energy states, accessed by tunneling. If we refer to the lower state of the resonant pair as the local ground state, the excitation energy density becomes  $n(\epsilon) = \frac{1}{k_B T_g} e^{-|\epsilon|/k_B T_g}$  ( $\epsilon > 0$ ). The partition function of a domain with an excitation energy  $\epsilon$ , possibly accompanied by populating vibrational states on top, is given by  $Z_\epsilon = 1 + e^{-\beta\epsilon} \prod_l Z_l^{2l+1}$ , where  $Z_l \equiv 1/(1 - e^{-\beta\hbar\omega_l})$  is the partition function of an  $l$ th order ripplon mode. Apart from the excitation  $\epsilon$ , we assume here each ripplon has a nearly harmonic spectrum. Note, our energy level scheme automatically insures that the atomic motions near the thermally inactive defects will only contribute to the regular lattice vibrations. The specific heat per domain, calculated from  $Z_\epsilon$  and averaged over  $n(\epsilon)$ , is shown in Fig.2.

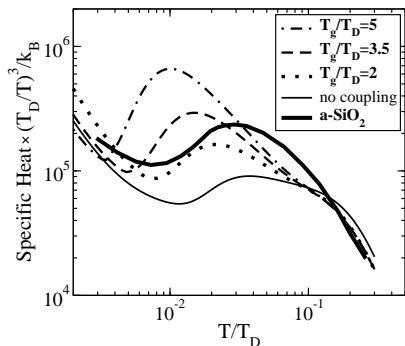


FIG. 2. The heat capacity per domain, as follows from the derived TLS + ripplon density of states, divided by  $T^3$ . This includes the Debye contribution. The thin line neglects phonon coupling and has  $T_g/T_D = 4$ . The experimental curve for amorphous silica from [17], originally given in  $\text{J/gK}^4$ , is shown multiplied by  $\hbar^3 \rho c_s^3 (6\pi^2) (\xi/a)^3 / k_B^4$ , where we used  $\omega_D = (c_s/a)(6\pi^2)^{1/3}$ ,  $(\xi/a)^3 = 200$  [8],  $\rho = 2.2 \text{ g/cm}^3$ ,  $c_s = 4100 \text{ m/sec}$  and  $T_D = 342 \text{ K}$  [2]. Using the appropriate value of  $k_B T_g / \hbar \omega_D = 4.4$  for a-SiO<sub>2</sub> would place the peak somewhat lower in temperature than observed.

In order to estimate the scattering by the domain tunneling accompanied by the ripplons and thus the heat conductivity, we need to know the effective scattering density of states, the transition amplitudes and

the coupling to the phonons. Any transition in the domain accompanied by a change in its internal state is coupled to the gradient of the elastic field with energy  $g \sim \rho c_s^2 \int d\mathbf{s} \cdot \mathbf{d}(\mathbf{r})$ , where  $\mathbf{d}(\mathbf{r})$  is the molecular displacement at the droplet edge due to the transition [8]. Therefore any transitions between groups marked with solid lines in Fig.1b are coupled to the phonons with the same strength as the underlying (TLS-like) transition, shown to be  $g \simeq \sqrt{k_B T_g \rho c_s^2 a^3}$  [8], and no selection rules apply for the change in the ripplon quantum numbers because of the strong anharmonicity. We do not possess detailed information on the transition amplitudes, however they should be on the order of the transition frequencies themselves, just as for those TLS's that are primarily responsible for the phonon absorption at the lower  $T$  whose transition amplitudes are also comparable to the total energy splitting.

Since all transitions couple equally to the phonons, we can now calculate the density of the scattering states. If  $\epsilon > 0$ , the phonon absorbing transition occurs from the ground state. The corresponding total number of ways to absorb a phonon of energy  $\hbar\omega$  is  $\rho(\omega) = \int_0^\infty d\epsilon n(\epsilon) \sum_{\{n_{lm}\}} \delta(\hbar\omega - [\epsilon + \sum_{lm} n_{lm} \hbar\omega_{lm}]) = 1/k_B T_g \sum_{\{n_{lm}\}} \theta(\omega - \sum_{lm} n_{lm} \hbar\omega_{lm}) e^{-\beta_g \hbar(\omega - \sum_{lm} n_{lm} \hbar\omega_{lm})}$ , where we sum over all occupation numbers of the ripplons with quantum numbers  $l, m$  ( $m = -l..l$ ). The transition may also occur from the higher energy conformational state ( $\epsilon < 0$  in Fig.1b), and we have to compute  $\rho(\omega)$  from these states too. To find  $\rho(\omega)$ , we compute the cumulative density of states  $N_E(\omega) \equiv \int_{-\infty}^0 d\epsilon \rho(\omega; -\epsilon < E) = \int_0^E d\epsilon n(\epsilon) \sum_{\{n_{lm}\}} \delta(\hbar\omega - [\sum_{lm} n_{lm} \hbar\omega_{lm} - \epsilon])$ . In a calculation parallel to obtaining  $Z_l$ , this can be evaluated using an integral representation of the step function  $\theta$  along with the use of steepest descent. The scattering from excited states is proportional to  $\rho_{exc}(\omega, T) \equiv \int_0^\infty dE f(E, T) \partial N_E(\omega) / \partial E$ , where  $f(E, T) \equiv 2/(e^{\beta\epsilon} + 1)$  gives the appropriate Boltzmann weights.

Accurate calculation of the heat conductivity requires solving a kinetic equation for the phonons coupled with the multilevel systems, which would account for saturation effects etc. We utilize instead a single relaxation time approximation for each phonon frequency. The Fermi golden rule yields for the scattering rate of a phonon with  $\hbar\omega \sim k_B T$  the relation  $\tau_\omega^{-1} \sim \omega \frac{\pi g^2}{\rho c_s^2} [\rho(\omega) + \rho_{exc}(\omega, T)]$ . The heat conductivity then equals  $\kappa = \frac{1}{3} \sum_\omega l_{mfp}(\omega) C_\omega c_s$ . The mean free path cannot be less than the phonon's wave-length  $\lambda$  (which occurs at the Ioffe-Riegel condition). We account for multiple scattering effects by putting  $l_{mfp} = c_s \tau_\omega + \lambda$ . At high  $T$ , the heat is not carried by "ballistic" phonons, but rather is transferred by a random walk from site to site, as originally anticipated by Einstein [18] for homogeneous isotropic solids.

The coupling of the multilevel excitations to phonons leads to significant frequency shifts and damping of the

resonant transitions. To compute these coupling effects, we replace the discrete summation over the different uncoupled harmonics  $\sum_l \int d\omega \delta(\omega - \omega_l)$  by integration over “lorentzian” profiles  $\sum_l \int d\omega \frac{\gamma_\omega/\pi}{[\omega - \omega_l(\omega)]^2 + \gamma_\omega^2}$ , where  $\gamma_\omega$  is a (frequency dependent) friction coefficient and  $\omega_l(\omega)$  is the renormalized ripplon frequency, which has been shifted due to the corresponding dispersion effects. The total relaxation rate of a transition involving more than one

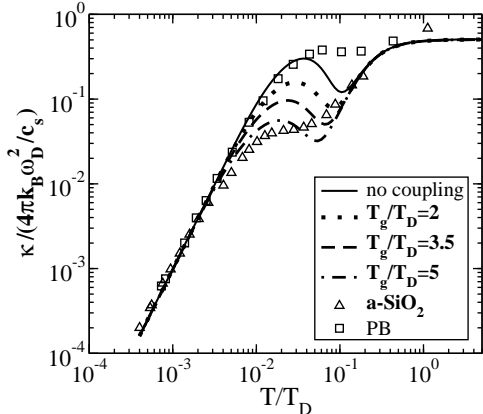


FIG. 3. The predicted low  $T$  heat conductivity. The “no coupling” case neglects phonon coupling effects on the ripplon spectrum. The (scaled) experimental data are taken from [19] for a-Si ( $k_B T_g/\hbar\omega_D \simeq 4.4$ ) and [2] for polybutadiene ( $k_B T_g/\hbar\omega_D \simeq 2.5$ ). The empirical universal lower  $T$  ratio  $l_{mfp}/l \simeq 150$  [2], used explicitly here to superimpose our results on the experiment, was predicted by the present theory earlier within a factor of order unity [8].

mode is thus the sum of the inverse life-times of the participating modes. This would be entirely correct for a frequency independent  $\gamma$ , but should be still an adequate approximation at the low  $T$  end of the plateau, where the absorption is mostly due to single ripplon mode processes. The mode decay rate  $\gamma_\omega$  is the phonon irradiation induced drag equal in the lowest order of perturbation to  $\gamma_\omega = \frac{g^2}{4\pi\rho c_s^2}(\omega/c_s)^3 \simeq \frac{3\pi}{2\hbar}k_B T_g(\omega/\omega_D)^3$ , where we do not distinguish between the longitudinal and transverse phonons. The corresponding (frequency dependent) ripplon frequency shift required by Kramers-Kronig relation gives a renormalized frequency  $\omega_l(\omega) = \omega_l - \frac{3}{2\hbar}k_B T_g(\omega_c/\omega_D)^3 f_0^{\omega_c} \frac{d\omega'(\omega'/\omega_c)^3}{\omega' - \omega}$ , where the principal value integral (numerically  $\sim 1$ ) is a slow (but sign-changing!) function of  $\omega$  and the cut-off frequency  $\omega_c$ .  $\omega_c$  is of the order (but greater than)  $(a/\xi)\omega_D$ , since the phonons with wave-length shorter than  $\xi$  cause an increasingly smaller effective gradient of the phonon field as sensed by a region of size  $\xi$ . Although our approximation for  $\gamma_\omega$  and  $\omega_l(\omega)$  should break down in detail for  $\omega \gtrsim \omega_c$ , it makes little difference computationally, as the damping is already very intense at this point. Both the frequency shift and the damping broaden the absorption peak, the former being quantitatively more important. While the peaks’ positions are determined by the quantum energy

scale  $\omega_D$ , the spectral *shifts* are proportional to  $T_g$ . The non-universality of the  $k_B T_g/\hbar\omega_D$  ratio, which varies over the range of 2 to 5, thus yields a non-universal position of the plateau. This is consistent with the experimentally observed material dependence in this regime. In Fig.3, we show the resultant heat conductivities for different values of the ratio  $k_B T_g/\hbar\omega_D$ , using the specific cutoff  $\omega_c = 1.8(a/\xi)\omega_D$ . The non-monotonic behavior exhibited by this approximation in the plateau region is likely an artifact of neglecting thermal saturation in the kinetic theory. Assuming heat transport is dominated by thermal phonons suggests  $\rho_{exc}(\omega, T) \rightarrow \rho_{exc}(\omega, \sim \hbar\omega/k_B)$ . This leads to a temperature independent  $l_{mfp}(\omega)$  and a strictly horizontal plateau.

The coupling effects on the heat capacity can be obtained by replacing each  $Z_l$  with the formula for a damped oscillator. The resulting bump in  $c/T^3$ , shown in Fig.2, is therefore also non-universal depending on  $k_B T_g/\hbar\omega_D$ , being smaller for organic glasses, as seen in experiment.

This work was supported by NSF grant CHE-9530680.

---

- [1] C.C.Yu and A.J.Leggett, *Comments Cond. Mat. Phys.*, **14**, 231 (1988); A.J.Leggett, *Physica B* **169**, 322 (1991).
- [2] J.J.Freeman and A.C.Anderson, *Phys. Rev. B* **34**, 5684 (1986).
- [3] P.W.Anderson, B.I.Halperin and C.M.Varma, *Philos. Mag.* **25**, 1 (1972).
- [4] W.A.Phillips, *J. Low Temp. Phys.* **7**, 351 (1972).
- [5] *Amorphous Solids: Low-Temperature Properties*, edited by W.A.Phillips, Springer-Verlag Berlin Heidelberg New York, 1981.
- [6] T.S.Grigera, V.Martín-Mayor, G.Parisi, and P.Verrocchio, *Phys. Rev. Lett.* **87**, 085502 (2001).
- [7] Yu.M.Galperin, V.G.Karpov, and V.I.Kozub, *Adv. Phys.* **38**, 669 (1991).
- [8] V.Lubchenko and P.G.Wolynes, *Phys. Rev. Lett.* **87**, 195901 (2001); cond-mat/0105307.
- [9] P.G.Wolynes, *Acc. Chem. Res.* **25**, 513 (1992); T.R.Kirkpatrick, D.Thirumalai, *Transp. Theor. Stat.Phys.* **24**, 927 (1995) and references therein.
- [10] Xiaoyu Xia and P.G.Wolynes, *PNAS* **97**, 2990 (2000); cond-mat/9912442.
- [11] E.V.Russel and N.E.Israeloff, *Nature* **408**, 695 (2000).
- [12] H.Silescu, *J.Non-Cryst. Solids* **243**, 81 (1999).
- [13] Xiaoyu Xia and P.G.Wolynes, *Phys. Rev. Lett.* **86**, 5526 (2001); cond-mat/0008432.
- [14] A.C.Anderson in [5] and references therein.
- [15] P.M.Morse and H.Feshbach, “*Methods of Theoretical Physics*”, McGraw-Hill, 1953; v.2 p.1469.
- [16] A.Wischnewski, U.Buchenau, A.J.Dianoux, W.A.Kamitakahara, J.L.Zaretsky, *Phys. Rev. B* **57**, 2663 (1998).
- [17] R.O.Pohl in [5].
- [18] A.Einstein, *Ann. Phys.* **35**, 679 (1911).
- [19] T.L.Smith, Ph.D. thesis, University of Illinois, 1974.